·Basic Research·

Heparanase−1 activities in the development of laser induced choroidal neovascularization

Wei-Qiang Tang[1], Bao-Ke Hou[2]

[1] Department of Ophthalmology, the First Affiliated Hospital of General Hospital of People's Liberation Army, Beijing 100048, China

[2] General Hospital of People's Liberation Army, Beijing 100853, China

Correspondence to: Wei-Qiang Tang. Department of Ophthalmology, the First Affiliated Hospital of General Hospital of People's Liberation Army, Beijing 100048, China. weiqiangtang2005@yahoo.com.cn

Abstract

● **AIM:** To investigate the role of heparanase−1 in laser−induced choroidal neovascularization (CNV).

● **METHODS:** Experimental CNV was induced by krypton laser photocoagulation in 15 male Brown Norway rats. Fundus fluorescein angiography and histopathological examination were performed in observing the CNV development. The expression and distribution of heparanase −1 protein in the laser lesions were determined by immunohistochemistry and western blotting analysis.

● **RESULTS:** The success rate of laser induced CNV was approximately 75% on 3 −4 weeks after laser photo − coagulation. The protein levels of heparanase −1 increased significantly in the retina−choroidal complex of CNV models when compared to normal rat eyes ($P<$ 0.01). Immunostaining confirmed strong heparanase −1 expressions in all laser lesions, and it displayed to be highest at the newly formed blood vessels within the fibrovascular complex in the subretinal space.

● **CONCLUSION:** Heparanase−1 is closely involved in the development of laser induced CNV.

● **KEYWORDS:** choroidal neovascularization; immunohisto-chemistry; western blotting; heparanase-1

INTRODUCTION

C horoidal neovascularization (CNV) correlates with a variety of ocular diseases, such as, exudative macular degeneration, angioid streaks and pathological myopia [1-3]. However, the molecular mechanisms involved in the CNV remain largely unknown [4]. Disruption of the barrier of Bruch's membrane leading to the growth of CNV from the choroid into the sub-RPE (retinal pigment epithelium) and subretinal spaces is thought to be the pathological basis [5]. Study has also suggested that endothelial cell migration and macrophage infiltration, which should be regulated by the degradation of extracellular matrix (ECM) barrier, are involved in the CNV [6].

It has been well known that heparan sulfate proteoglycan (HSPG) is a key component of basement membranes and ECM, which is constituented with multiple heparan sulphate (HS) side chains linked to a core protein, and the HS polysaccharide chains in the ECM bind and regulate the activities of many growth factors [7-9]. Heparanase-1 is the only mammalian endoglycosidase known that specifically cleaves HS side chains of HSPG [10]. This study was to verify whether heparanase-1 expression is correlated to the development of CNV.

MATERIALS AND METHODS

Laser −induced CNV model Eighteen male adult Brown Norway rats weighing 200-230g were purchased from Vital River Laboratory Animal Technology Co. Ltd. (Beijing, China). All experiments with 18 rats were conducted in accordance with the ARVO Statement for the Use of Animals in Ophthalmic and Vision Research. The rats were anesthetized with an intraperitoneal injection of 10% chloral hydrate (3mL/kg), and the pupils were dilated with 1% tropicamide eye drops. CNV was induced with a krypton laser (Novua2000 krypton laser equipment, Coherent Inc., USA) in both eyes of 15 rats, 6 eyes of 3 rats were sampled as normal controls. 20 laser spots (50-μm spot size, 0.05-second duration and 360-mw powers) with acute vapor bubbles were placed in the ocular fundus around the optic nerve of each eye (Figure 1X).

Fluorescein angiography On day 2, 4, 7, 14, 21, and 28 after laser photocoagulation, induced-CNV lesions were studied by fluorescein angiography. The anesthetized rats were intraperitoneally injected with 10% fluorescein sodium (3mL/kg), and angiograms were obtained 5-6 minutes after the injection. The formation of CNV was confirmed by the presence of fluorescein leakage.

Histological and immunohistochemical staining On day 3, 7,

14, 21, 28, and 56 after photocoagulation, rats were euthanized by cervical dislocation and eyes were enucleated and fixed at 4% Paraformaldehyde solution, followed by embedding in paraffin. Serial 5μm thick slices were cut and were firstly subjected to Hematoxylin and Eosin (HE) staining and immunohistochemistry analysis. After endogenous peroxidase activity was quenched by 3% hydrogen peroxide and blocking with goat serum for 20 minutes, the sections were incubated with the polyclonal rabbit anti-heparanase-1 primary antibody (1:100; Santa Cruz Biotechnology, Santa Cruz, CA, USA) at 4℃ overnight. Rinsed with PBS and then incubated with goat polyclonal secondary antibody to rabbit IgG-HRP (1:250; Abcam Ltd., Hong Kong, China) for 30 minutes at room temperature. Color reaction was performed with a 3-amino-9-ethylcarbazole (AEC) substrate (Santa Cruz Biotechnology, Santa Cruz, CA, USA) for 10 minutes at room temperature. Finally, the sections were counterstained with Mayers hematoxylin. Negative controls were performed with PBS as the primary antibody.

Western blot analysis On day 28 after laser photocoagulation, 3 CNV model rats and 3 normal control rats were euthanized by cervical dislocation and eyes were enucleated. Harvested retina-choroidal complex were homogenized individually into $1 \times$PBS lysis buffer and centrifuged at $15\ 000 \times$g at 4℃ for 15 minutes. The total protein concentration of each sample was normalized using the Bradford method. An equal volume of $2 \times$SDS loading buffer was added to each applied 30μg protein sample, which was then subjected to boiling for 3 minutes. Cooled to room temperature before separating by 12.5% SDS-polyacrylamide gels and transferred to polyvinylidene fluoride (PVDF) membranes. The membranes were then blocked with 5% fat-free milk in Tris-buffered saline plus 0.05% Tween-20 ($1 \times$TBST) overnight at 4℃. The next day, the membranes were then incubated with the primary antibody of rabbit anti-heparanase-1 (1:500; Santa Cruz Biotechnology, Santa Cruz, CA, UAS) and rabbit anti-GAPDH (1:1000; BGI Tech Solutions Co., Ltd., Beijing, China) at 4℃ overnight. After washing in $1 \times$TBST three times, the membranes were incubated with a horseradish peroxidase-conjugated secondary antibody (1:1000; ZSGB-BIO Biotechnology Co., Ltd. Beijing, China) for 60 minutes at 37℃. They were washed again in $1 \times$TBST thoroughly, and immunoreactivity was visualized by incubating in enhanced chemiluminescence reagents (APPLYGEN Biotechnology Co., Ltd. Beijing, China) for 2 minutes. The immuno-reactivity signals were quantified by densitometry, and the relative changes in heparanase-1 levels were represented as the ratio of the optical density value between heparanase-1 and GAPDH.

Statistical Analysis The quantitative data were expressed as the means±SD and analyzed using a paired t-test analysis, $P<0.05$ was considered statistically significant.

RESULTS

Fluorescein Leakage from Laser Induced CNV Lesions
FFA revealed hyperfluorescence of the laser spots on day 2 after photocoagulation and no fluorescence leakage on day 4 (Figure 1A, B). It also showed that the fluorescence leakage at the laser spots was firstly observed on day 7 after photocoagulation (Figure 1C), and a total of 137 (26.3%) CNV fluorescence leaking lesions in 13 rats were seen. The numbers of leaking lesions at day 14 increased to 287 (71.8%) in 10 rats (Figure 1D). On day 21 and 28 after laser photocoagulation, the numbers of leaking lesions were 211 (75.3%) in 7 rats and 150 (75.0%) in 5 rats separately (Figure 1E, F).

Histological and Heparanase −1 Immunostaining
Histological analysis confirmed that induced CNV began to form on day 7 after photocoagulation (Figure 2A). Damages to the retinal pigment epithelium (RPE), photoreceptors, outer nuclear layer, outer plexiform layer and the inner nuclear layer were seen in all CNV lesions resulted from disruption of the Bruch's membrane. The newly formed fibrovascular complex, which consisted of collagen fibers, fibroblasts, endothelial cells, RPE cells and newly formed vessels, extended towards the subretinal space. Within the fibrovascular complex, the number and size of new vessels increased continuously and reached a maximum at 28 days (Figure 2B). 56 days after photocoagulation, CNV lesions filled with more collagen fibers surrounding vessels (Figure 2C).

Immunohistochemistry study disclosed that heparanase-1 staining were strongly detectable in the laser lesions after photocoagulation. In early phase, heparanase-1 staining tended to be diffuse in the laser spots, but in the late phase the distribution of heparanase-1 staining was showed to be highest at the newly formed vessels within the fibrovascular complex in the subretinal space. (Figure 2D, E, F).

Heparanase −1 protein levels On 28 days after photocoagulation, 3 CNV models and 3 normal control rats were sacrificed and 12 eyes were processed for western blotting studies. Low-level expression of 50kDa heparanase-1 protein was seen in the normal retina-choroidal complex. Notably enhanced protein bands were found in the retina-choroidal complex of CNV (Figure 3). The relative level of heparanase-1 protein was 0.891±0.357 (normal controls) and 1.996±0.087 (CNV models) separately. There was a significant up-regulation of heparanase-1 protein in laser induced CNV (t=7.366, $P<0.01$).

DISCUSSION
The current study showed the relationship between heparanase-1 and laser induced CNV development. Heparanase-1, an endoglycosidase that cleaves heparan
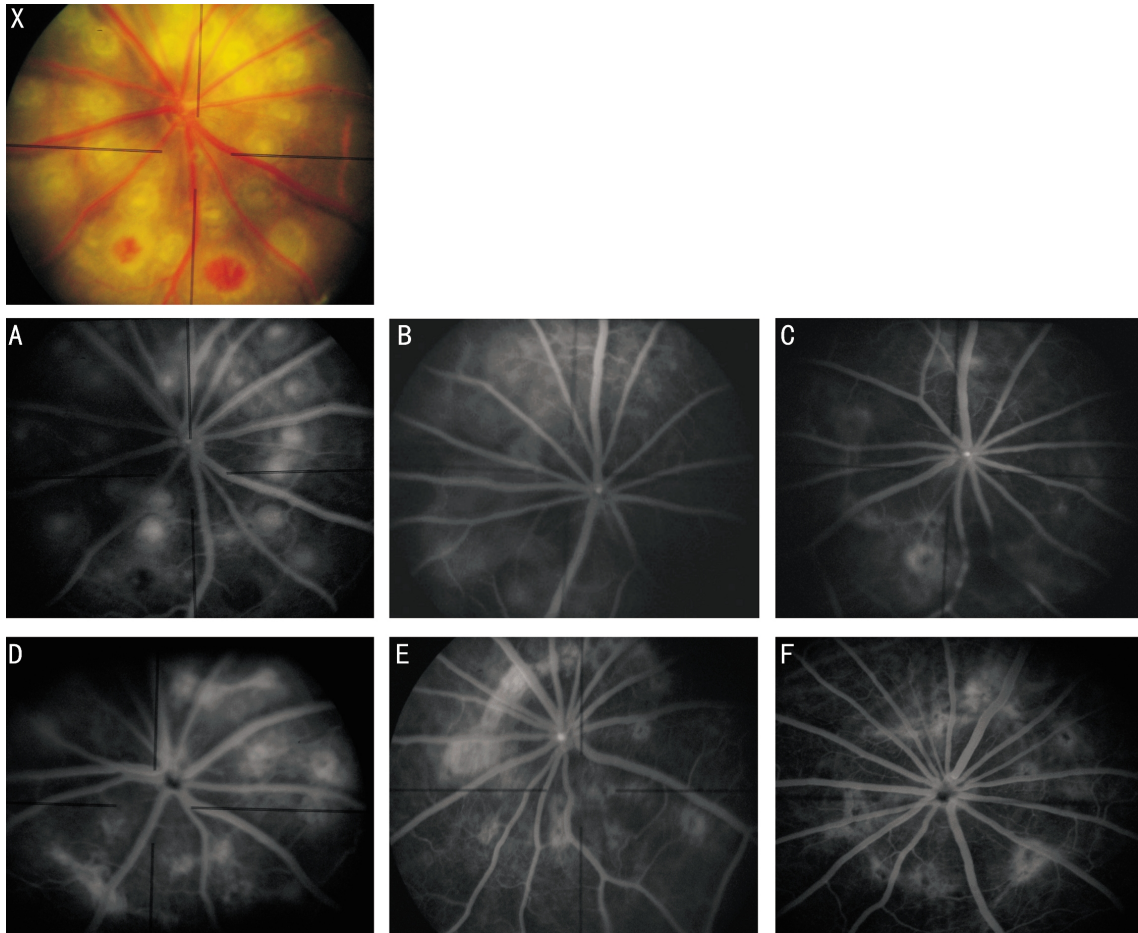
Figure 1 Laser photocoagulation and Dynamic observation of CNV leakage by fluorescein angiography X: 20 laser spots with acute vapor bubbles were placed in the fundus around the optic nerve for inducing CNV; A: On day 2 after photocoagulation, it showed hyperfluorescence of laser spot size; B: On day 4, no fluorescence leakage of the laser spots were seen; C: Few CNV fluorescence leakage were seen on day 7; D, E, F: Rats developed more CNV leakage on day 14, 21 and 28 when compared to those on day 7.
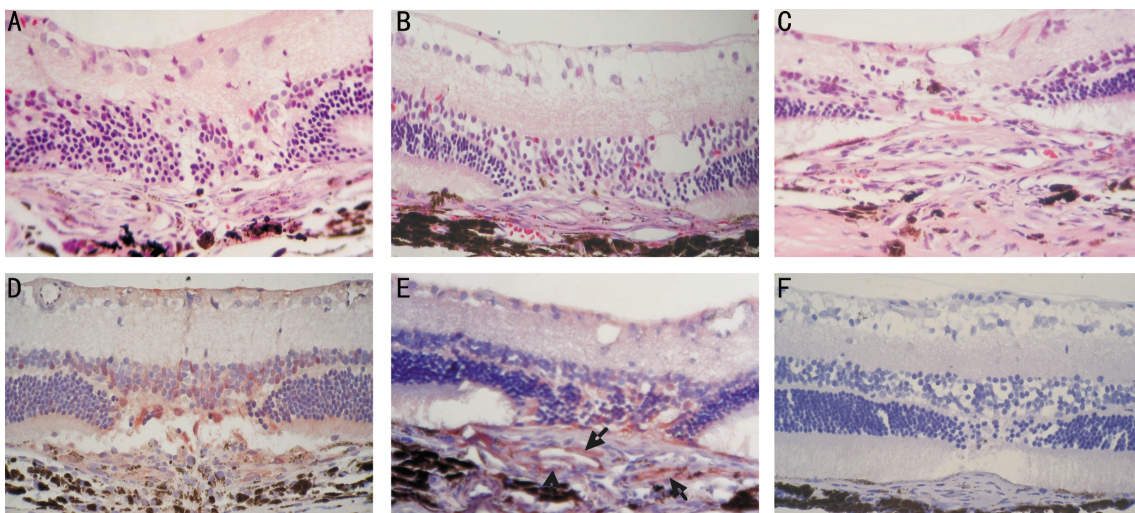
Figure 2 CNV observed by histopathology and heparanase−1 staining by immunohistochemistry A: 7 days after photocoagulation, a fully developed fibrovascular complex formed (HE×400); B: Newly formed vessels increased both in number and size on day 28 (HE×400); C: CNV lesion contained more collagen fibers on day 56 (HE×400); D: 3 days after photocoagulation, heparanase-1 positive staining diffuse in the laser lesion (IHC×400); E: 28 days after photocoagulation, heparanase-1 positive staining in CNV lesion, black arrows showed the highest staining at the newly formed vessels (IHC×400). F: Negative control (IHC×400).

sulfate side chains, is demonstrated in embryo development, hair growth, wound healing, and inflammation [11]. Moreover, accumulated studies have suggested that heparanase-1 is up-regulated in many malignancies and correlates with tumor invasion, metastasis, and angiogenesis [12]. Heparanase-1 may stimulate the tumor angiogenesis *via* releasing the
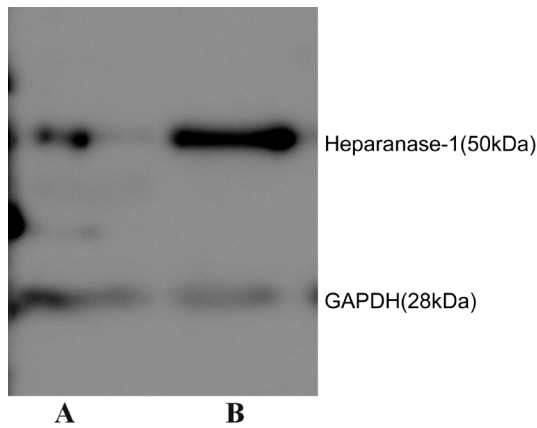
Figure 3 Western blotting analysis of the heparanase −1 protein in CNV. GAPDH was blotted as a control and indicated no changes between two groups A: Normal control; B: CNV model.

heparin-binding growth factors such as vascular endothelial growth factor (VEGF) [13]. Xu *et al* [14] reported that heparanase-1 and VEGF expression were positively correlated with the microvessel density in human adrenocortical carcinoma. Additional study showed that heparanase-1 is involved in hypoxia-induced retinal neovascularization [15]. As laser induced CNV shares many of the same pathologic steps with tumor angiogenesis and neovascularization arises from varied causes [16,17], heparanase-1 may contribute to the similar mechanism in them.

We generated the laser induced CNV model by a rupture of Bruch's membrane in concordance with previous reports [18,19], and the success rate of CNV which was demonstrated by the fundus fluorescence angiography was approximately 75% on 3-4 weeks after laser photocoagulation. In addition, laser lesions showed the progressive subretinal ingrowth of new vessels from the early onset on 7 days up to peak on 28 days after photocoagulation, and the persistant neovascularization surrounded by more fibrinogen on 56 days. Therefore, the laser induced CNV model is best suited for studying the pathogenesis of CNV [20,21].

Using this CNV model, our study showed that the expression of 50 kDa heparanase-1 was significantly increased in the retina-choroidal complex submitted to laser-induced CNV but there was a low expression level in the retina-choroidal complex of normal rat. Liang *et al* [22] also reported that a 50 kDa heparanase-1 levels were significantly increased in a mouse model of oxygen-induced retinopathy and closely related with the VEGF levels in retinal vascular endothelial cells. It has been confirmed that heparanase-1 is initially synthesized as an inactive 65 kDa pro-enzyme form, undergoing proteolytic cleavage to yield an N-terminal 8kDa subunit and a C-terminal 50kDa subunit. The 50kDa subunit is required for HS side chains cleavage [23,24]. Thus, the

elevated expression of 50 kDa protein suggested that heparanase-1 had been activated in the process of CNV development.

Our study also displayed strong immunohistochemical staining of heparanase-1 in both early laser lesions and CNV lesions after 7 days. 3 days after laser photocoagulation, the positive heparanase-1 signals distributed diffusely within the laser spots, indicating that the enzyme plays a role in the activity of macrophages, neutrophils, RPE cells and endothelial cells seen in histological sections. Several studies have demonstrated that these diffusely infiltrating cells and resident cells in the sites of laser injury promoted the early development of neovascularization [25-27]. Furthermore, we found that the heparanase-1 positive staining tended to be highest at the newly formed blood vessels within the fibrovascular complex in the subretinal space. This observation might be explained by the fact that heparanase-1 was secreted by endothelial cells under an inflammatory condition of the laser induced CNV [28]. Taken together, heparanase-1 is involved in the development of laser induced CNV, elevated heparanase-1 levels may promote the migration and proliferation of infiltrating cells and resident cells in the retina-choroidal complex by directly disrupting the ECM or indirectly by releasing HS-binding growth factors.

In summary, our study shows that activated heparanase-1 levels is elevated in the laser induced CNV, and contributes to the migration and proliferation of infiltrating cells and resident cells in the retina-choroidal complex. This study may provide the basis for heparanase-1 as a new target in the treatment of CNV.

REFERENCES

1 Ates O, Azizi S, Alp HH, Kiziltunc A, Beydemir S, Cinici E, Kocer I, Baykal O. Decreased serum paraoxonase 1 activity and increased serum homocysteine and malondialdehyde levels in age−related macular degeneration. *Tohoku J Exp Med* 2009;217(1):17−22

2 Mitry D, Zambarakji H. Recent trends in the management of maculopathy secondary to pathological myopia. *Graefes Arch Clin Exp Ophthalmol* 2012;250(1):3−13

3 Liu YC, Yang CS, Shyong MP, Lee FL, Lee SM. Intravitreal injection of bevacizumab for the treatment of choroidal neovascularization in a patient with angioid streaks. *J Chin Med Assoc* 2009;72(2):98−102

4 Kume T. Ligand−dependent Notch signaling in vascular formation. *Adv Exp Med Biol* 2012;727:210−222

5 Chong NH, Keonin J, Luthert PJ, Frennesson CI, Weingeist DM, Wolf RL, Mullins RF, Hageman GS. Decreased thickness and integrity of the macular elastic layer of Bruch's membrane correspond to the distribution of lesions associated with age−related macular degeneration. *Am J Pathol*

2005;166(1):241-251

6 Fujimura S, Takahashi H, Yuda K, Ueta T, Iriyama A, Inoue T, Kaburaki T, Tamaki Y, Matsushima K, Yanagi Y. Angiostatic effect of CXCR3 expressed on choroidal neovascularization. *Invest Ophthalmol Vis Sci* 2012;53(4):1999-2006

7 Kim SH, Turnbull J, Guimond S. Extracellular matrix and cell signaling: the dynamic cooperation of integrin, proteoglycan and growth factor receptor. *J Endocrinol* 2011;209(2):139-151

8 Reiland J, Sanderson RD, Waguespack M, Barker SA, Long R, Carson DD, Marchetti D. Heparanase degrades syndecan-1 and perlecan heparan sulfate: functional implications for tumor cell invasion. *J Biol Chem* 2004; 279(9):8047-8055

9 Symes K, Smith EM, Mitsi M, Nugent MA. Sweet cues: How heparan sulfate modification of fibronectin enables growth factor guided migration of embryonic cells. *Cell Adh Migr* 2010;4(4):507-510

10 Roy M, Marchetti D. Cell surface heparan sulfate released by heparanase promotes melanoma cell migration and angiogenesis. *J Cell Biochem* 2009;106(2):200-209

11 Augusto TM, Rosa-Ribeiro R, Carvalho HF. Neonatal exposure to high doses of 17β -estradiol results in inhibition of heparanase-1 expression in the adult prostate. *Histochem Cell Biol* 2011;136(5):609-615

12 Yuan L, Hu J, Luo Y, Liu Q, Li T, Parish CR, Freeman C, Zhu X, Ma W, Hu X, Yu H, Tang S. Upregulation of heparanase in high-glucose-treated endothelial cells promotes endothelial cell migration and proliferation and correlates with Akt and extracellular-signal-regulated kinase phosphorylation. *Mol Vis* 2012;18:1684-1695

13 Xu X, Ding J, Rao G, Shen J, Prinz RA, Rana N, Dmowski WP. Estradiol induces heparanase-1 expression and heparan sulphate proteoglycan degradation in humanendometrium. *Hum Reprod* 2007;22(4): 927-937

14 Xu YZ, Zhu Y, Shen ZJ, Sheng JY, He HC, Ma G, Qi YC, Zhao JP, Wu YX, Rui WB, Wei Q, Zhou WL, Xie X, Ning G. Significance of heparanase-1 and vascular endothelial growth factor in adrenocortical carcinoma angiogenesis: potential for therapy. *Endocrine* 2011;40 (3): 445-451

15 Hu J, Song X, He YQ, Freeman C, Parish CR, Yuan L, Yu H, Tang S. Heparanase and vascular endothelial growth factor expression is increased in hypoxia-induced retinal neovascularization. *Invest Ophthalmol Vis Sci* 2012;53(11):6810-6817

16 El Bradey M, Cheng L, Bartsch DU, Appelt K, Rodanant N, Bergeron-Lynn G, Freeman WR. Preventive versus treatment effect of AG3340, a potent matrix metalloproteinase inhibitor in a rat model of choroidal neovascularization. *J Ocul Pharmacol Ther* 2004;20(3):217-236

17 Dai C, Liu G, Li L, Xiao Y, Zhang X, Lu P. ADP-ribosylation factor as a novel target for corneal neovascularization regression. *Mol Vis* 2012;18: 2947-2953

18 Wang JH, Jiang W, Kang ZF, Liang LN, Liu XM, Tian NN, Zhang Q. Study of krypton laser-induced choroidal neovascularization in a Guinea pig model of high anisometropia. *Yan Ke Xue Bao* 2012;27(2):76-81

19 Ming Y, Algvere PV, Odergren A, Berglin L, van der Ploeg I, Seregard S, Kvanta A. Subthreshold transpupillary thermotherapy reduces experimental choroidal neovascularization in the mouse without collateral damage to the neural retina. *Invest Ophthalmol Vis Sci* 2004;45 (6): 1969-1974

20 Toma HS, Barnett JM, Penn JS, Kim SJ. Improved assessment of laser-induced choroidal neovascularization. *Microvasc Res* 2010;80 (3): 295-302

21 Lee E, Rewolinski D. Evaluation of CXCR4 inhibition in the prevention and intervention model of laser-induced choroidal neovascularization. *Invest Ophthalmol Vis Sci* 2010;51(7):3666-3672

22 Liang XJ, Yuan L, Hu J, Yu HH, Li T, Lin SF, Tang SB. Phosphomannopentaose sulfate (PI-88) suppresses angiogenesis by downregulating heparanaseand vascular endothelial growth factor in an oxygen-induced retinal neovascularization animal model. *Mol Vis* 2012; 18:1649-1657

23 Ilan N, Elkin M, Vlodavsky I. Regulation, function and clinical significance of heparanase in cancer metastasis and angiogenesis. *Int J Biochem Cell Biol* 2006;38(12):2018-2039

24 McKenzie EA. Heparanase: a target for drug discovery in cancer and inflammation. *Br J Pharmacol* 2007;151(1):1-14

25 Tsutsumi-Miyahara C, Sonoda KH, Egashira K, Ishibashi M, Qiao H, Oshima T, Murata T, Miyazaki M, Charo IF, Hamano S, Ishibashi T. The relative contributions of each subset of ocular infiltrated cells in experimental choroidal neovascularisation. *Br J Ophthalmol* 2004;88 (9): 1217-1222

26 Zhou J, Pham L, Zhang N, He S, Gamulescu MA, Spee C, Ryan SJ, Hinton DR. Neutrophils promote experimental choroidal neovascularization. *Mol Vis* 2005;11:414-424

27 Li ZR, Li YP, Lin ML, Su WR, Zhang WX, Zhang Y, Yao L, Liang D. Activated macrophages induce neovascularization through upregulation of mmp-9 and VEGF in rat corneas. *Cornea* 2012;31(9):1028-1035

28 Chen G, Wang D, Vikramadithyan R, Yagyu H, Saxena U, Pillarisetti S, Goldberg IJ. Inflammatory cytokines and fatty acids regulate endothelial cell heparanase expression. *Biochemistry* 2004;43(17):4971-4977